FTIR Characterization of the Reactive Interface of Cobalt Oxide Nanoparticles Embedded in Polymeric Matrices

Rina Tannenbaum,*,† Melissa Zubris,† Kasi David,† Dan Ciprari,† Karl Jacob,‡,§ Iwona Jasiuk,⊥ and Nily Dan#

School of Materials Science and Engineering, School of Polymer, Textile and Fiber Engineering, School of Mechanical Engineering, Georgia Institute of Technology, Atlanta, Georgia, Department of Mechanical Engineering, Concordia University, Montreal, Quebec, Canada, and Department of Chemical Engineering, Drexel University, Philadelphia, Pennsylvania

Received: August 10, 2005; In Final Form: December 6, 2005

Fourier transform infrared spectroscopy (FTIR) was used as a novel characterization method to determine the properties of the interface that developed when cobalt oxide nanoparticles were self-assembled in a poly(methyl methacrylate) (PMMA) matrix. The method employed the distinct changes that were observed in the infrared spectra of the polymer upon adsorption onto the cobalt oxide nanoparticles, allowing a quantitative determination of the average number of contact points that the average polymer chain formed with the surface of a cobalt oxide nanoparticle of average size. The results obtained with this method compared favorably to those obtained by the coupling of transmission electron microscopy (TEM) experiments with thermogravimetric analysis (TGA). On the basis of both methods, we concluded that the interfacial region created between the cobalt oxide nanoparticles and PMMA is extremely sensitive to the chain length, i.e., the number of anchor points and the density of the polymer layer increase with chain molecular weight. At molecular weights of ∼250 000, the density of the polymer layer saturates at a value that correspond to that of very thin PMMA films.

1. Introduction

Nanostructured materials consist of phases with dimensions in the nanometer size range (1 to 100 nm). This is the range where atomic and molecular phenomena strongly influence the macroscopic material properties. It has been shown that the mechanical,[1−3] electronic,[4−6] magnetic,[6−8] and optical properties of a material vary as a function of the nanoscale domain size, while they are less sensitive to the size of micron-scale domains. As a result, composite materials in which nanoparticles,[6,9−16] nanofibers, or nanotubes[17−20] are dispersed in a matrix of another material, frequently display different material properties than composites based on larger particles.[21−26]

The definition of nanocomposite materials encompasses a large variety of systems made of distinctly dissimilar components, where at least one component of the composite has nanometer size dimensions.[17−26] The general class of organic/inorganic nanocomposite materials is a fast growing area of research. Significant effort has been focused on the ability to obtain control of the structure of nanoscale materials in the composite via innovative synthetic approaches.[28−34]

The properties of nanocomposite materials depend not only on the properties of their individual components but also on their organization in the composite as well as their interfacial characteristics. The latter is especially important in these systems where the ratio between the surface area and the volume is high. Indeed, several studies indicate that nanocomposites can display new properties which are not present in the constituent parent materials.[1−8]

One of the key factors influencing the macroscopic material behavior of composites, e.g., the load transfer between matrix and filler,[35−38] is the interfacial region between these two components. Reducing the size of filler while preserving the filler volume fraction leads to a dramatic increase of the volume fraction of the interfacial region (interphase). The interfacial region in a polymer nanocomposite, depicted schematically in Figure 1a, has distinct structural features, depending on the strength of the interactions between the filler particles and the polymer matrix. A weak attractive interaction will result in the extension of the polymer chains into the bulk polymer matrix, creating a diffuse interface, as shown in Figure 1b. Conversely, a strong attractive interaction involves the effective adsorption of polymer chains onto the surface of the fillers via bonding of functional groups of the polymer with reactive sites on the surface of the nanofillers.[39] Such an interaction will result in a flat (i.e., dense) configuration of the polymer on the surface of the nanofillers and a compact interface, as shown in Figure 1c. In addition, the strength of the interaction of a polymer molecule with the surface of the filler controls also the polymer molecular conformations and resulting interactions (e.g., entanglement distribution) in a larger region surrounding the filler (as shown in Figure 1a). Thus, control of the particle/polymer interface will enable control of the mechanical and structural properties of the nanocomposite materials.

As shown in Figure 1, the particle/polymer interface may be characterized through several parameters such as the number of "adsorbed" chains (namely, chains that have at least one segment in contact with the particle), the thickness of the

* Address correspondence to this author. E-mail: rina.tannenbaum@mse.gatech.edu.
† School of Materials Science and Engineering, Georgia Institute of Technology.
‡ School of Polymer, Textile and Fiber Engineering, Georgia Institute of Technology.
§ School of Mechnaical Engineering, Georgia Institute of Technology.
⊥ Department of Mechanical Engineering, Concordia University
Department of Chemical Engineering, Drexel University.

10.1021/jp054469y CCC: $33.50
Published on Web 01/19/2006

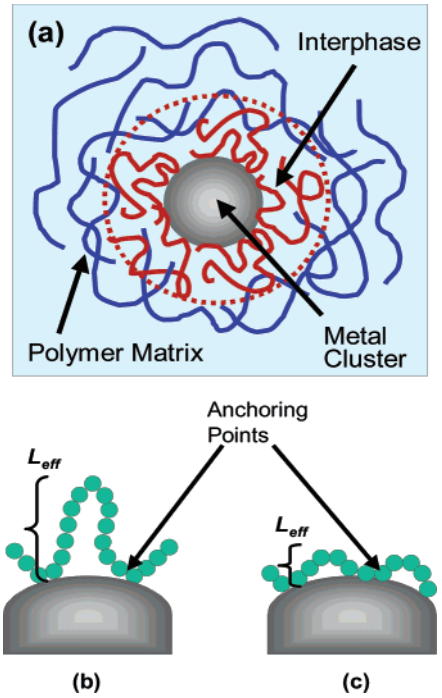

Figure 1. Schematic representation of a metal−polymer nanocomposite: (a) The various components in a metal−polymer nanocomposite highlighting the presence of the extended interfacial region, i.e., the interphase. (b) A detailed schematic view of the adsorption characteristics on the surface of the cobalt oxide clusters of a weakly binding polymer, in which most of the segments reside in loops. (c) A detailed schematic view of the adsorption characteristics on the surface of the cobalt oxide clusters of a strongly binding polymer, in which most of the segments reside on the surface.

adsorbed layer, and the number of contacts between the particle and the polymer. We have previously developed a method that uses transmission electron microscopy images (TEM) coupled with thermal gravimetric analysis (TGA) data to characterize the average thickness of the adsorbed polymer chains on a nanoparticle surface, L_{eff} (as in Figure 1b,c), and subsequently determine the number of contact points (anchors) between the adsorbed polymer and the nanoparticle.[40] The method consists of the determination of the average cluster diameter, D, from TEM images, and the calculation of L_{eff} from TGA measurements of the coated nanoparticles (after all physisorbed polymer chains have been removed by repeated washing). The average volume of the monolayer of chemisorbed polymer chains on each cluster is given by $V_{poly} = m_{sample}w_{poly}/N_{cluster}\rho_{poly}$, where w_{poly} is the mass fraction of the polymer moiety in the sample as determined from TGA measurements, $N_{cluster}$ is the total number of nanoclusters in the sample, and ρ_{poly} is the density of a thin film of the polymer matrix used in a given nanocomposite system.[35] Since the volume of a polymer-coated nanocluster, V_{tot}, is the sum of the volumes of the metallic and polymeric moieties, the following expression can be developed:

$$V_{tot} = V_{cluster} + V_{poly} = \frac{4\pi}{3}\left(\frac{D + 2L_{eff}}{2}\right)^3 \quad (1)$$

The expression $D + 2L_{eff}$ denotes the diameter of a polymer-coated nanoparticle as shown by the dotted red circle in Figure 1a. Therefore, it is possible to calculate L_{eff}, the effective thickness of the polymer layer, as follows:

$$L_{eff} = \frac{1}{2}\left[\frac{6w_{poly}MW_{cluster}\epsilon}{\pi\rho_{poly}w_{cluster}N_A}\left(\frac{D_{cluster}}{d_{metal}}\right)^3 + {D_{cluster}}^3\right]^{1/3} - \frac{D_{cluster}}{2} \quad (2)$$

Assuming that the polymer behaves as a freely jointed chain between the contact points (i.e. bonds) with the metal cluster surface, and neglecting bridging chains (polymer chains adsorbed on multiple clusters), we can calculate the minimum number of segments in an average chain residing in loops as $n_{loop} \propto (L_{eff})^2$, and consequently, the maximum number of contact points per chain as $n_{anchor} = N/n_{loop}$, where N is the average number of segments per chain.

We have found that for a given polymer molecular weight, fewer contact points lead to a high concentration of polymer loops and a diffuse interfacial region, while a larger number of contact points leads to a high concentration of polymer trains and a compact interfacial region.[40] This in turn has a direct impact on the density of the interphase and its contribution to the mechanical properties of the nanocomposite.

The main drawback of the TEM/TGA method is the fact that it requires some assumptions regarding the density of the adsorbed polymer monolayer. In this paper we focus on the development of a new characterization method of the interfacial structure based on infrared spectroscopy. This method will allow the direct calculation of n_{anchor} without the need to assume the density of the adsorbed polymer monolayer. On the contrary, it will serve as a direct method for the determination of the density of the adsorbed layer. We recognize that this will be possible only in systems in which the adsorption of the polymer chains onto the metal oxide nanoclusters generates a characteristic infrared signature as a result of new bond formation at the interface, i.e., due to reactive chemisorption, and cannot be applied to physisorbed polymer chains where the adsorption process occurs via dipole interactions.

In this paper we chose to focus on poly(methyl methacrylate) (PMMA) as the polymeric matrix, with the reinforcing nanoparticles being cobalt oxide nanoparticles that were formed in situ in the polymer matrix from homogeneously dispersed organometallic cobalt precursors. The guiding principle for the choice of this nanoparticle/polymer system is the distinct changes that are observed in the infrared spectra of the polymer upon adsorption onto the cobalt oxide nanoparticles, allowing a quantitative determination of the average number of contact points that the average polymer chain forms with the cluster surface. Finally, we will compare the two characterization systems and evaluate the implications regarding the structure of the polymer−metal cluster interfacial region.

2. Experimental Methods

2.1. Synthesis of the Nanocomposites. Forty five milliliters of a 2 wt % solution of poly(methyl methacrylate), PMMA (Alfa Aesar), of $\bar{M}_w = 30\,000$, 60 000, 120 000, 250 000, or 330 000 (first two with PDI = 1.04, and the last three with PDI = 1.12) in chlorobenzene was added to a three-neck, jacketed reaction flask, followed by the addition of 45 mL of a 1×10^{-2} M solution of $Co_2(CO)_8$ in chlorobenzene. The combined solution had final PMMA and $Co_2(CO)_8$ concentrations of 1 wt % and 5×10^{-3} M, respectively. The reaction flask was flushed with dry N_2 and an aliquot was removed for Fourier transform infrared spectroscopy (FTIR) analysis. The decomposition was carried out at 90 °C with constant stirring for ca. 10 h. The reaction was deemed complete when all infrared carbonyl absorption bands of $Co_2(CO)_8$ have disappeared. This process

TABLE 1: Average Sizes of the Cobalt Oxide Nanoparticles Formed in Solutions of Poly(methyl methacrylate) of Various Polymer Molecular Weights

molecular weight of PMMA	av particle diameter (nm)
30 000	67 ± 12
60 000	50 ± 8
120 000	28 ± 8
250 000	27 ± 5
330 000	31.5 ± 5

resulted in the formation of Co_2O_3 and some CoO nanoparticles suspended in a poly(methyl methacrylate) solution. The average particles sizes of cobalt oxide nanoparticles formed in solutions of PMMA with different molecular weights are summarized in Table 1. To form nanocomposite films, a small amount of polymer solution containing the already-formed nanoparticles was deposited on a glass slide and the solvent was allowed to evaporate slowly in a temperature-controlled oven at 90 °C for a week. The volume fraction of the oxide nanoparticles in the nanocomposite films was (1.6 ± 0.3)%.

2.2. Characterization of the Nanocomposites. Thermogravimetric analysis (TGA) was conducted to measure the thickness of the polymer interphase for the PMMA nanocomposites. TGA samples were prepared by centrifuging an aliquot of a previously reacted solution containing cobalt oxide nanoclusters capped with PMMA, with $\bar{M}_w$ = 120 000, 250 000, and 330 000, using an Eppendorf Concentrator 5301 Centrifuge, at 12 000−17 000 rpm. This separated excess solvent from the polymer-coated nanoclusters. The supernatant chlorobenzene solution was removed, and the remaining particles were washed with both chlorobenzene and hexane to remove any excess unbound polymer or partially reacted cobalt carbonyl fragments. The suspension was centrifuged again and the process was repeated three times. Upon completion, a fraction of the isolated PMMA-coated particles were placed into a TGA pan and the data were collected with a TA Instruments TGA Model 50.

Transmission electron microscopy (TEM) was performed to allow the determination of the average size of the cobalt nanoparticles formed and provide the basis for the TEM/TGA analysis of the interfacial structure of the PMMA nanocomposites and the calculations of the adsorbed PMMA layer density. TEM samples were obtained by placing a small droplet of the reacted solution containing the polymer-coated cobalt particles onto a Formvar-coated copper TEM grid from Ted Pella. The grid rested on a thin piece of tissue paper so that the liquid will drain into the paper leaving a very thin film on the grid itself. The TEM analysis was performed on a JEOL 4000EX high-resolution electron microscope with an operating voltage of 200 keV.

Finally, another fraction of the isolated PMMA-coated particles (described previously) was mixed with a drop of Nujol mull to form a thick paste, cast on an NaCl circular crystal, and analyzed by means of transmission FTIR, using Nicolet Nexus 870, at a resolution of 2 cm^{-1} and 3000 scans. The infrared spectra of very thin films of PMMA spin-coated on gold surfaces were used as a reference, representing a nonreactive interface. The details of the preparation of these samples have been previously described elsewhere.[41−43]

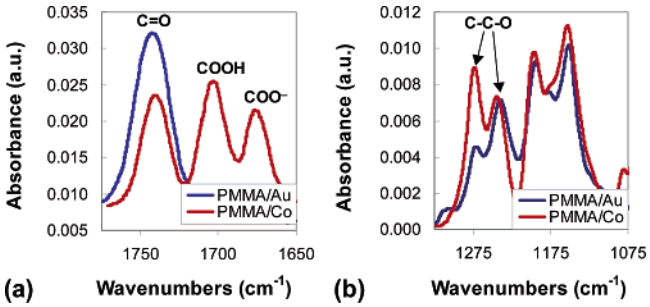

Figure 2. (a) The infrared absorption bands of PMMA in the carbonyl spectral region at 1743, 1702, and 1674 cm^{-1}, corresponding to the stretch of the C═O groups, the stretch of the hydrogen-bonded COOH groups, and the asymmetric stretch of the COO^- groups, respectively. (b) The changes of the relative intensities of the 1241 and 1271 cm^{-1} infrared bands, corresponding to the cooperative symmetric and antisymmetric stretches of the C−C−O groups, respectively, indicating changes in the conformation of the polymer at the surface of the cobalt oxide clusters. The spectrum of a very thin spin-coated PMMA layer on Au is used as a reference.

3. Results and Discussion

The nanocomposites were synthesized via an in situ synthesis consisting of the thermal decomposition of organometallic precursors in the presence of polymer as previously described.[39,40] This method allows the control of particle size via the variations of polymer concentration in the original reaction solution. The system examined consisted of cobalt oxide nanoclusters formed in the presence of PMMA. It has been previously shown[39] that under the reaction conditions, PMMA interacts vigorously with the surface of the cobalt clusters, resulting in a strong adsorption. This interaction occurs in two steps, as shown in eq 3.

In the first step, a fraction of the ester bonds in the polymer are hydrolyzed in the presence of the cobalt oxide nuclei to form carboxylic acid groups.[39,41,42] In the second step, some of these carboxylic groups undergo dissociation to form the carboxylate anionic group. The formation of the carboxylate anion has been shown to occur only upon formation of a bond (anchoring point) at the surface of the cobalt oxide nanoparticle, and hence it can be considered as a quantitative measure of the number of anchoring points per polymer chain.[39,43] The concentration of the carboxylate anion in a given sample can be obtained via the evolution of the 1674 cm^{-1} infrared absorption band, corresponding to the asymmetric stretch of the COO^- group, as shown in Figure 2a. It is important to remember that in the case of PMMA, the strong interactions with the cobalt oxide surface will promote extensive bonding, which will result in the loss of entropy and changes in the conformation of the polymer due to chain confinement on the surface. The changes in the

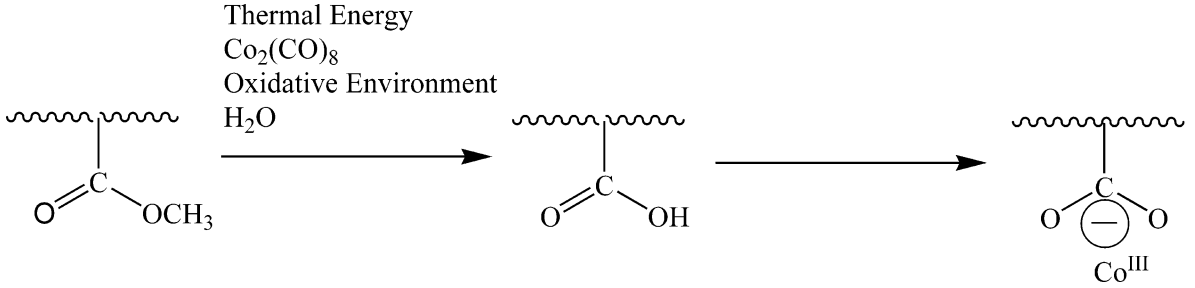

(3)

TABLE 2: Calculations of the Thickness of the Adsorbed Polymer Layer and the Resulting Number of Polymer Anchoring Points for the System of Co_2O_3 Nanoclusters Embedded in a Poly(methyl methacrylate) Matrix, Based on Experimental Results Obtained from FTIR Measurements and the TEM/TGA Method for Selective Systems

mol wt of PMMA	no. of polymer chains in sample	$E_{1674}/E_{1743} \times E_{1241}/E_{1271}$	no. of reacted groups	no. of anchoring points/chain by FTIR (±35)	no. of anchoring points/chain by TEM/TGA (±40)
30 000	2.1×10^{18}	0.061	1.9×10^{19}	9.2	N/A
60 000	1.0×10^{18}	0.091	2.8×10^{19}	27.5	N/A
120 000	5.2×10^{17}	0.270	8.0×10^{19}	155.7	160.1
250 000	2.5×10^{17}	0.252	7.8×10^{19}	315.7	289.0
330 000	1.9×10^{17}	0.282	8.7×10^{19}	466.1	414.8

conformation of the polymer at the surface can be directly observed by following the changes of the relative intensities of the 1241 and 1271 cm^{-1} infrared bands, corresponding to the cooperative symmetric and antisymmetric stretches of the C−C−O group, respectively, and shown in Figure 2b. The characteristic changes in the infrared spectrum of PMMA upon its reactive adsorption on the surface of the cobalt oxide nanoclusters[41−43] allow the quantitative analysis of the extent of this adsorption based solely on spectral information, without the need of prior assumptions. The ratio of the 1241 and 1271 cm^{-1} infrared absorption bands gives a direct indication as to the fraction of functional groups that have been affected by the conformational changes of the polymer chain due to adsorption. Multiplying this ratio by the absorbance intensity of the 1674 cm^{-1} infrared absorption band, and by the number of monomers in the sample, and normalizing the result by the intensity of the initial adsorption of the C═O bond at 1743 cm^{-1} (acting as an internal standard), will give the total number of PMMA ester groups that have undergone hydrolysis followed by dissociation and anchoring. The quotient of the total number of adsorbed carboxylate groups, N_{COO^-}, and the total number of chains in the sample, N_{chain}, shown below in eq 4, will give the average number of anchoring points per chain, as summarized in Table 2.

$$\text{no. of anchors/chain} = \frac{N_{COO^-}}{N_{chains}} = \frac{E_{1674}}{E_{1743}}\frac{E_{1241}}{E_{1271}}\frac{N_{monomers}}{N_{chains}} \quad (4)$$

When comparing the number of anchoring points for the samples containing PMMA with $\bar{M}_w = 120\,000$, 250 000, and 330 000 obtained from infrared intensities with the number of anchoring points of the same samples that were calculated using the combination of TEM and TGA, summarized in Table 2 as well, the results seem to be in very good agreement.

As previously observed with the PS-cobalt system, in which the polymer is weakly bonded to the cluster surface via dipole interactions,[40] the extent of polymer adsorption on the cluster surface is dependent on the molecular weight of the polymer. The same is also true in the case of PMMA, as shown in Figure 3a. As the molecular weight of the polymer chain increases, so does the number of anchor points per chain However, the number of anchor points per chain increases more rapidly with PMMA molecular weight, and so the fraction of adsorbed segments increases as well. It is interesting to note that in the limit of high molecular weight the effect of chain length becomes more or less linear, so that the fraction of adsorbed segments is similar for molecular weights where $\bar{M}_w > 120\,000$.

The use of the infrared spectroscopic method for the characterization of the structure of the cluster−polymer interfacial region allows the independent determination of the density of the adsorbed polymer layer, as shown in Figure 3b. The density is calculated by dividing the mass of the adsorbed polymer layer (obtained from the number of reacted segments) by the volume of the adsorbed polymer layer (obtained from the effective thickness of the adsorbed layer, L_{eff}, and the average particle size, $D_{cluster}$, via the expression

$$V_{poly} = \frac{4\pi}{3}\left[\left(\frac{D_{cluster}}{2} + L_{eff}\right)^3 - \left(\frac{D_{cluster}}{2}\right)^3\right]$$

We see that the density of the adsorbed layer (Figure 3b) increases with the chain length, or with the number of anchor points per chain (Figure 3a). This is as expected. If all segments would have adsorbed, then the density should have reached that of bulk polymer. Thus, it is not surprising that increasing the number of anchoring points (through increase in chain length) would lead to an increase in the interphase density.

However, we find that even though only a small fraction of the chains is anchored (≤20%), in the limit of high molecular weight chains, the density of the interphase saturates at a value of 1.26 g/cm^3. This value is consistent with the previously measured density of very thin PMMA films (<20 nm), 1.28 g/cm^3.[45] The fact that the density of thin films is higher than the density of bulk PMMA (1.19 g/cm^3) is most likely an overestimate due to the sharp transition between the density of the adsorbed PMMA film and that of the Co_2O_3 nanocluster, as observed on silica substrates.[45]

The sharp increase in the number of anchoring points per chain with molecular weight in PMMA differs from the case of PS, where the number of anchoring points per chain increases linearly with molecular weight.[40] To understand the difference between the two polymers we must refer to the parameters controlling polymer adsorption onto solid substrates:[44] The formation of an anchor point between a chain in solution and a solid surface reduces the chain translational entropy, while gaining in interaction energy. Further adsorption of segments from that same chain would reduce the conformational entropy of the chain, while further increasing the gain due to interaction energy. In the case of PS, the energetic gain due to PS/Co association is small. As a result, the adsorbed polymer chains do not deform significantly and the number of anchor points is proportional to their length. In the case of PMMA, the gain associated with anchoring is high, so that chains that are already confined to the particle surface deform to form even more contacts, leading to the increased sensitivity of anchor points to chain length. In the limit where the molecular weight of the PMMA chains is high, however, the particle surface becomes saturated (as given by the high interphase density), which leads to a leveling off as seen in Figure 3c.

4. Summary

In this paper we have shown that in the case of strongly binding polymers, such as PMMA, FTIR may be used as an independent method for the characterization of the interfacial structure, provided that the new bonds that developed at the interface between the polymer and the metal oxide cluster surface gave rise to a characteristic new infrared absorption

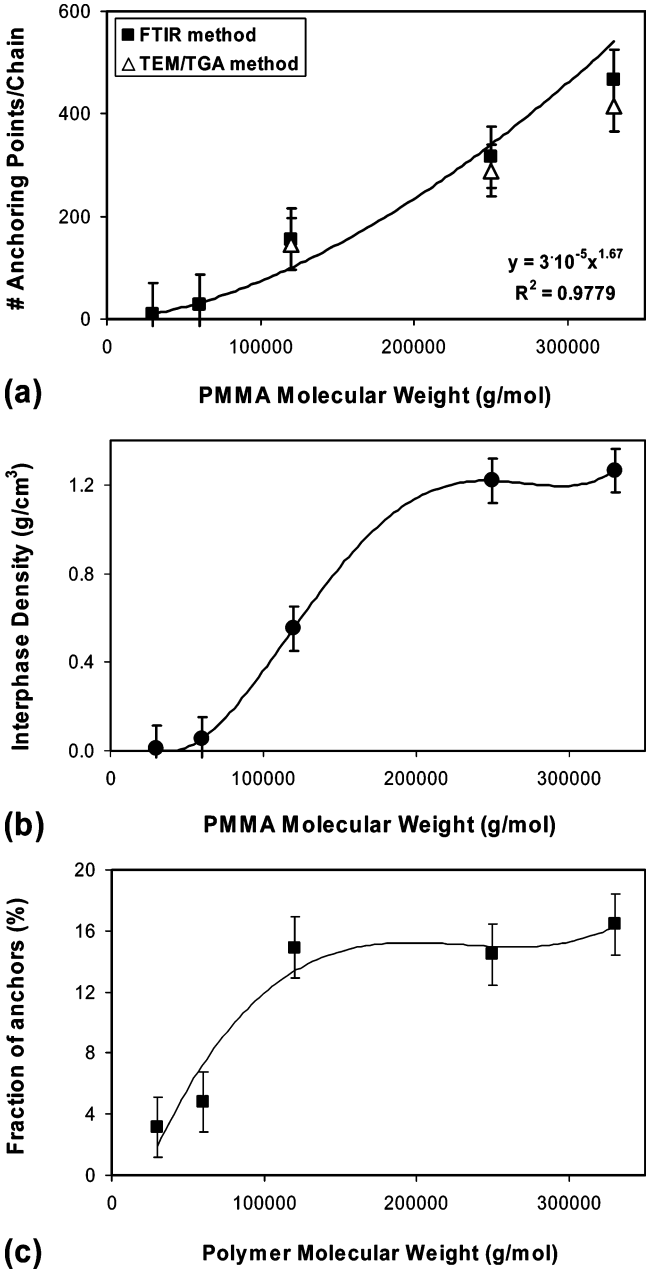

Figure 3. The structure of the interface between PMMA and cobalt clusters: (a) The number of anchoring points for a Co_2O_3/PMMA system as a function of polymer molecular weight, calculated from the experimental results obtained from the FTIR experiments together with the results using the TEM/TGA method for selective systems. In this case, the number of anchoring points scale with $\bar{M}_w^{5/3}$. (b) The calculated density of the adsorbed polymer monolayer for the Co_2O_3/PMMA system as a function of polymer molecular weight. (c) The fraction of the segments in the PMMA chains that are directly bonded to the surface of the cobalt clusters as a function of polymer molecular weight.

band. The results obtained form this spectroscopic method compare favorably with the results obtained by the indirect TEM/TGA method and hence, where applicable, this method may prove very useful, especially since it does not require any assumptions regarding the density of the adsorbed polymer layer.

Moreover, our results show that the properties of the adsorbed layer, or interphase, are extremely sensitive to the polymer chain molecular weight. The number of anchor points per chain, namely, polymer segments that are in direct contact with the metal nanoparticle, increases with the chain molecular weight to the power of ~1.7 (Figure 3a, anchors/chain $\propto \bar{M}_w^{5/3}$). This is in contrast to the case of weakly adsorbing PS, where the number of anchor points increases linearly with chain length.[40] The increase in the number of PMMA anchor points correlates to an increase in the interphase density, which saturates at a value that corresponds to a thin PMMA film (Figure 3b). The effect of polymer chain length on the structure of the interphase layer can be understood in terms of an adsorption model, where the number of anchor points and density of the adsorbed layer are a function of the strength of interactions between the nanoparticle and the polymer.

Acknowledgment. This work was supported by the Petroleum Research Fund, administered by the American Chemical Society, PRF #40014-AC5M.

Note Added after ASAP Publication. This manuscript was originally published on the Web January 19, 2006 with an incorrect value in Table 1 due to production error. The corrected version of this manuscript was reposted January 20, 2006.

References and Notes

(1) Lane, R. A.; Craig, B. D.; Neergaard, L. *Adv. Mater. Proc. Technol.* **2002**, *i-ix*, 1−49.
(2) Neralla, S.; Kumar, D.; Yarmolenko, S.; Sankar, J. *Composites B* **2004**, *35*, 157−162.
(3) Cypes, S. H.; Saltzman, W. M.; Giannelis, E. P. *J. Controlled Relat.* **2003**, *90*, 163−169.
(4) Cendoya, I.; Lopez, D.; Alegria, A.; Mijangos, C. *J. Polym. Sci. Polym. Phys.* **2001**, *39*, 1968−1975.
(5) Flahaut, E.; Peigney, A.; Laurent, C.; Marliere, C.; Chastel, F.; Rousset, A. *Acta Mater.* **2000**, *48*, 3803−3812.
(6) Li, J.; Gao, L.; Guo, J. *J. Eur. Ceram. Soc.* **2003**, *23*, 69−74.
(7) Lopez, D.; Cendoya, I.; Torres, F.; Tejada, J.; Mijangos, C. *Polym. Eng. Sci.* **2001**, *41*, 1845−1852.
(8) Lopez, D.; Cendoya, I.; Torres, F.; Tejada, J.; Mijangos, C. *J. Appl. Polym. Sci.* **2001**, *82*, 3215−3222.
(9) Thilly, L.; Lecouturier, F.; Coffe, G.; Peyrade, J. P.; Askenazy, S. *IEEE Trans. Appl. Superconduct.* **2000**, *10*, 1269−1272.
(10) Ash, B. J.; Rogers, D. F.; Wiegand, C. J.; Schadler, L. S.; Siegel, R. W.; Banicewicz, B. C.; Apple, T. *Polym. Composites* **2002**, *23*, 1014−1025.
(11) Kim, Y. W.; Mitmoto, M. *J. Mater. Sci.* **2000**, *35*, 5885−5890.
(12) Huerta, A.; Calderon, H. A.; Yee-Madeira, H.; Umemoto, M.; Tsuchiya, K. *Proc. Mater. Res. Soc. Symp.* **2000**, *581*, 253−258.
(13) Thilly, L.; Lecouturier, F.; Von Stebut, *J. Acta Mater.* **2002**, *50*, 5049−5065.
(14) Ji, X.; Hampsey, J. E.; Hu, Q.; He, J.; Yang, Z.; Lu, Y. *Chem. Mater.* **2003**, *15*, 3656−3662.
(15) Veron, M.; Ludwig, O.; Lecouturier, F. *Mater. Sci. Eng. A* **2001**, *309−310*, 510−513.
(16) Qiang, X.; Chunfang, Z.; JianZun, Y.; Cheng, S. *J. Appl. Polym. Sci.* **2004**, *91*, 2739−2749.
(17) Lau, K. T.; Chipara, M.; Ling, H. Y.; Hui, D. *Composites B* **2004**, *35*, 95−101.
(18) Valentini, L.; Biagiotti, J.; Kenny, J. M.; Lopez-Manchado, M. A. *J. Appl. Polym. Sci.* **2003**, *89*, 2657−2663.
(19) Bai, J. B.; Allaoui, A. *Composites A* **2003**, *34*, 689−694.
(20) Penumadu, D.; Dutta, A.; Pharr, G. M.; Files, B. *J. Mater. Res.* **2003**, *18*, 1849−1853.
(21) Young, S. K.; Mauritz, K. A. *J. Polym. Sci. Polym. Phys.* **2001**, *39*. 1282−1295.
(22) Veprek, S.; Argon, A. S. *J. Vac. Sci. Technol. B* **2002**, *20*, 650−664.
(23) Agag, T.; Koga, T.; Takeichi, T. *Polymer* **2001**, *42*, 3399−3408.
(24) Kovacevic, V.; Lucic, S.; Leskovac, M. *J. Adhes. Sci. Technol.* **2002**, *16*, 1343−1365.
(25) Ishak, Z. A. M.; Chow, W. S.; Ishiaku, U. S.; Karger-Kocsis, J.; Apostolov, A. A. *J. Appl. Polym. Sci.* **2004**, *91*, 175−189.
(26) Hao, J.; Yuan, M.; Deng, X. *J. Appl. Polym. Sci.* **2002**, *86*, 676−683.
(27) Sheng, N.; Boyce, M. C.; Parks, D. M.; Rutledge, G. C.; Abes, J. I.; Cohen, R. E. *Polymer* **2004**, *45*, 487−506.
(28) Wilson, J. L.; Poddar, P.; Frey, N. A.; Srikanh, H.; Mohomed, K.; Harmon, J. P.; Kotha, S.; Wachsmuth, J. *J. Appl. Phys.* **2004**, *95*, 1439−1443.
(29) Werndrup, P.; Verdenelli, M.; Chassagneux, F.; Parola, S.; Kessler, V. G. *J. Mater. Chem.* **2004**, 14, 344−350.

(30) Pacheco, F.; Gonzalez, M.; Medina, A.; Velumani, S.; Ascencio, J. A. *Appl. Phys. A* **2004**, *78*, 531−536.
(31) Percy, M. J.; Michailidou, V.; Armes, S. P.; Perruchot, C.; Watts, J. F.; Greaves, S. J. *Langmuir* **2003**, *19*, 2072−2079.
(32) Ni, Y.; Ge, X.; Zhang, Z.; Ye, O. *Mater. Lett.* **2002**, *55*, 171−174.
(33) Clapsaddle, B. J.; Gash, A. E.; Satcher, J. H., Jr.; Simpson, R. L. *J. Noncrystal. Solids* **2003**, *331*, 190−201.
(34) Huang, X.; Brittain, W. J. *Macromolecules* **2001**, *34*, 3255−3260.
(35) Wahab, M. A.; Ha, C. S. *Comput. Interface* **2003**, *10*, 475−488.
(36) Kovacevic, V.; Lucic, S.; Leskovac, M. *J. Adhes. Sci. Technol.* **2002**, *16*, 1343−1365.
(37) Kovacevic, V.; Leskovac, M.; Lucic, B. S. *J. Adhes. Sci. Technol.* **2002**, *16*, 1915−1929.
(38) Smith, G. D.; Bedrov, D.; Li, L.; Byutner, O. *J. Chem. Phys.* **2002**, *117*, 9478−9490.
(39) King, S.; Hyunh, K.; Tannenbaum, R. *J. Phys. Chem. B* **2003**, *107*, 12097−12104.
(40) Tadd, E. H.; Zeno, A. D.; Zubris, M.; Dan, N.; Tannenbaum, R. *Macromolecules* **2003**, *36*, 6497−6502.
(41) Kostandinidis, F.; Thakkar, B.; Chakraborty, A. K.; Potts, L.; Tannenbaum, R.; Tirrell, M.; Evans, J. *Langmuir* **1992**, *8*, 1307−1317.
(42) Tannenbaum, R.; Hakanson, C.; Zeno, A. D.; Tirrell, M. *Langmuir* **2002**, *18*, 5592−5599.
(43) Tannenbaum, R.; King, S.; Lecy, J.; Tirrell, M.; Potts, L. *Langmuir* **2004**, *20*, 4507−4514.
(44) Netz, R. R.; Andelman, D. *Phys. Rep.* **2003**, *380*, 1−95.
(45) van der Lee, A.; Hamon, L.; Holl, Y.; Grohens, Y. *Langmuir* **2001**, *17*, 7664−7669.